IEEE Access
Multidisciplinary : Rapid Review : Open Access Journal

Digital Object Identifier

Unified Implementation and Cross-Validation of the Integral Equation-Based Formulations for the Characteristic Modes of Dielectric Bodies

SHAODE HUANG[1,2], JIN PAN[1], CHAO-FU WANG[2], (Senior Member, IEEE), YUYUE LUO[1,3], AND DEQIANG YANG[1].

[1]School of Electronic Science and Engineering, University of Electronic Science and Technology of China, Chengdu 611731, China.
[2]Temasek Laboratories, National University of Singapore, Singapore 117411.
[3]School of Electrical and Data Engineering, University of Technology Sydney, Australia.

Corresponding author: Jin Pan (e-mail: jpuestc@163.com).

The part of this work conducted by Shaode Huang, Jin Pan, Yuyue Luo and Deqiang Yang was supported by the Foundation for Innovative Research Group of the National Natural Science Foundation of China under Grant 61721001.

ABSTRACT Theory of characteristic modes (TCM) can provide physical insight into the radiation mechanism of arbitrarily-shaped electromagnetic objects. However, how to compute the characteristic modes (CMs) of different structures is still an open problem. Even for the calculation of CMs of an isolated dielectric body, there are eleven integral equation (IE)-based formulations which result in different modal solutions. Such kind of non-uniqueness of solutions makes CMs community confused. One of the objectives of this paper is to outline the differences among all existing IE-based formulations for the CMs of dielectric bodies. The existing formulations are briefly reviewed and carefully compared. We present a procedure to implement the different formulations in a unified manner. Then, we make a complete comparison of the numerical results of existing methods for a dielectric cylinder, which also serves as cross-validation for these approaches. We hope that this paper will help researchers understand the calculation of CMs of dielectric bodies and explore the computation methods of CMs for more complex objects.

INDEX TERMS Characteristic modes, dielectric body, integral equation, implementation, cross-validation.

I. INTRODUCTION

The characteristic modes (CMs) form a special set of basis functions which can help identify the inherent resonant behaviors of arbitrarily-shaped objects. The CMs decomposition was firstly introduced as a set of modes diagonalizing the scattering matrix [1], [2]. It was subsequently reformulated by diagonalizing the impedance matrix of the electric field integral equation (EFIE) for the conducting bodies [3], [4]. Following the strategy of [3], the theory of CMs (TCM) was extended to the dielectric bodies using the volume integral equation (VIE) [5], named here as the VIE-based TCM. However, the VIE-based TCM results in heavy computational burden when the electric size of the object increases. A surface integral equation (SIE)-based TCM was proposed to alleviate the computation burdens [6]. Unfortunately, it was observed that the SIE-based TCM proposed in [6] resulted in spurious modes [7]. Many modified SIE-based TCM formulations had been subsequently come up to claim to be immune from spurious modes [8]–[13]. However, it was observed that some of the modified formulations provided different resonant modes. Such observation makes the CMs community confused as the results of different approaches should be similar if they are reasonable. More importantly, there is no complete comparison of existing CMs formulations up to now. The lack of comparison makes it hard to confirm whether these formulations are reliable. Recently, the TCM has been extended to the composite metallic-dielectric objects [13]–[18]. Note that the formulations in [13]–[18] are combinations of CMs formulation for conducting bodies in [3] and CMs formulations for dielectric bodies in [5], [9]–

[12]. Because the CMs formulations of dielectric bodies may give different modal solutions, the formulations in [13]–[18] should encounter the same problem. For instance, it was reported that the results of formulations in [14]–[16] were quite different [16].

This paper aims to outline the differences among all existing integral equation (IE)-based TCM formulations of dielectric bodies. Comprehensive literature survey tells us that there are eleven different IE-based TCM formulations for dielectric bodies in total [5], [6], [9]–[13]. They can be classified into two categories, i.e., the VIE-based TCM [5] and the SIE-based TCM [6], [9]–[13]. We can obtain eight SIEs based on the surface equivalence principle [19]. The eight SIEs are related to five basic operators. We find that all the ten SIE-based TCM formulations can be derived using different combinations of the five operators and can be conveniently implemented in a unified manner with using these five basic operators. Also it is helpful for researchers to understand and distinguish the ten different formulations. Then, we present a comprehensive comparison of the numerical results of existing formulations for a dielectric cylinder, in which the modal behaviors of the first 100 modes are displayed and compared. The eigenvalue curves, resonant frequencies, degeneracy, field distributions, radiation patterns, and computational efficiencies are carefully compared. The numerical results provide a cross-validation of the existing CMs formulations of dielectric bodies. We find that all existing approaches are capable of providing the reasonable resonant modes, but some of them result in extra modes. Besides, the modal behaviors of several formulations are very similar, which indicates that they might be more reasonable. The numerical results presented here can also serve as a benchmark test for future new CMs formulations of dielectric bodies.

II. REVIEW OF EXISTING FORMULATIONS

In this section, we briefly review the existing CMs formulations of dielectric bodies. Because of the limited space of the paper, we focus on the computation methods and numerical results but ignore their physical meanings. More details about the physical meanings can be found in the listed references. The existing CMs formulations can be classified into two groups, i.e., the VIE-based TCM and the SIE-based TCM. The VIE-based TCM is more robust but time-consuming than the SIE-based TCM. The SIE-based TCM formulations may result in spurious modes, which are caused by either the lack of the dependence relationships between electric and magnetic currents [20] or the improper choice of the weighting operators of the generalized eigenvalue equations [13]. Extra efforts must be made to suppress spurious modes in the SIE-based TCM.

A. VIE-BASED TCM

Referring to Fig. 1, let us consider a scattering problem with incident field $\left(\vec{E}^{inc}, \vec{H}^{inc}\right)$ illuminating a dielectric body whose permittivity and permeability are ϵ_d and μ_0, respectively. The region occupied by the dielectric body is denoted as V_d, and the boundary surface of V_d is denoted as ∂V_d. Stimulated by the incident field, there is induced volumetric polarization current $\vec{J}_v$ inside the dielectric, as shown in Fig. 1. The induced current generates the scattered field, and the total field is the sum of the incident field and the scattered field. Applying the volume equivalence principle [21], the induced current is related to the total field by the constitutive relationship

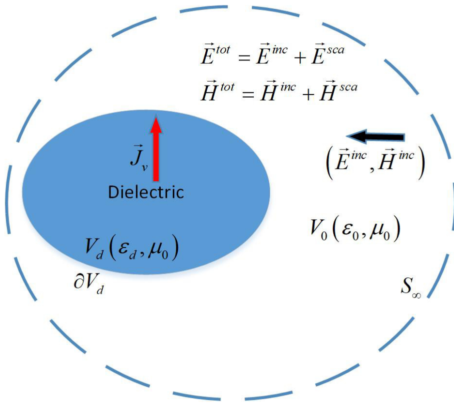

FIGURE 1: The induced volumetric polarization current of a dielectric body illuminated by incident field.

$$\vec{J}_v = j\omega\left(\varepsilon_d - \varepsilon_0\right)\left(\vec{E}^{inc} + \vec{E}^{sca}\right) = j\omega\Delta\varepsilon\vec{E}^{tot} \tag{1}$$

in which ω is the angular frequency. The induced current generates the scattered field according to [21]

$$\vec{E}^{sca} = -j\omega\mathbf{L_0}\left(\vec{J}_v\right) \tag{2}$$

where $\mathbf{L_0}$ is a linear operator which depends only on the shape of the volume V_d:

$$\mathbf{L_0}\left(\vec{X}\right) = \left(1 + \frac{1}{k_0^2}\nabla\nabla\cdot\right)\int_\Omega G_0\left(\vec{r}, \vec{r}^{\,\prime}\right)\vec{X}\left(\vec{r}^{\,\prime}\right)d\Omega^{\prime} \tag{3}$$

in which k_0 and G_0 are the wave number and Green's function in the background media. Substituting (2) into (1), we have the following VIE

$$\mathbf{Z}\left(\vec{J}_v\right) = \vec{E}^{inc} \tag{4}$$

where

$$\mathbf{Z} = j\omega\mathbf{L_0} + \left(j\omega\Delta\varepsilon\right)^{-1}\cdot\mathbf{I} \tag{5}$$

in which $\mathbf{I}$ represents the identity operator. Then the VIE-based TCM formulation is defined by [5]

$$\mathbf{X}\left(\vec{J}_n\right) = \lambda_n\mathbf{R}\left(\vec{J}_n\right) \tag{6}$$

in which $\mathbf{X}$ and $\mathbf{R}$ are Hermitian parts of $\mathbf{Z}$ as $\mathbf{Z} = \mathbf{R} + j\mathbf{X}$, where

$$\begin{cases}\mathbf{R} = \dfrac{1}{2}\left(\mathbf{Z} + \mathbf{Z}^H\right)\\ \mathbf{X} = \dfrac{1}{2j}\left(\mathbf{Z} - \mathbf{Z}^H\right)\end{cases} \tag{7}$$

IEEE Access
Multidisciplinary : Rapid Review : Open Access Journal

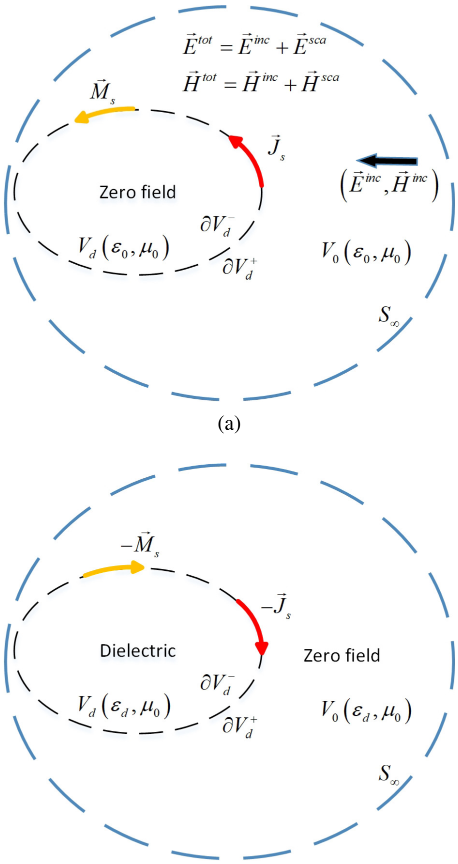

FIGURE 2: Surface equivalence principle. (a) External equivalent problem. (b) Interior equivalent problem.

in which $(\cdot)^H$ represents the conjugate transpose. Note that the $\mathbf{X}$ and $\mathbf{R}$ are also the imaginary and real parts of $\mathbf{Z}$ when $\mathbf{Z}$ is symmetric.

B. SIE-BASED TCM

In addition to the VIE-based TCM, the CMs of dielectric bodies can be obtained using the SIE-based TCM to alleviate computational burdens. Although the SIE-based TCM formulations require less computational resources than the VIE-based TCM, the procedures to acquire the SIE-based TCM formulations are more complicated than that of the VIE-based TCM. Extensive literature survey shows that there are ten different SIE-based TCM formulations in total [6], [9]–[13]. However, there is no comprehensive comparison of the existing SIE-based TCM formulations. In this section, we review the ten different SIE-based TCM formulations. We find that all the ten formulations can be derived using five basic operators and implemented in a unified manner.

Considering the surface equivalence principle [19], the problem in Fig. 1 can be divided into two subproblems, as shown in Fig. 2. In the first subproblem, the total field inside the dielectric body is assumed to be zero; meanwhile, the total field outside the dielectric body remains unchanged, as displayed in Fig. 2a. Note that the media property of V_d can be replaced with (ϵ_0, μ_0) in this subproblem according to the surface equivalence principle. Thus the entire space becomes an infinite homogeneous space with media parameters (ϵ_0, μ_0) [19]. There are equivalent electric and magnetic currents located on the surface of the dielectric body, according to the boundary conditions of the electromagnetic field. The surface equivalence principle indicates that the equivalent electric and magnetic currents generate the scattered filed outside the dielectric body and are responsible for the zero field inside the dielectric body [19]. Therefore, the following four SIEs can be obtained:

$$\vec{E}^{sca}\left(\vec{r}\right) = -j\omega\mu_0\mathbf{L_0}\left(\vec{J}_s\right) - \mathbf{K_0^-}\left(\vec{M}_s\right), \vec{r} \in \partial V^+ \quad (8)$$

$$\vec{H}^{sca}\left(\vec{r}\right) = -j\omega\varepsilon_0\mathbf{L_0}\left(\vec{M}_s\right) + \mathbf{K_0^-}\left(\vec{J}_s\right), \vec{r} \in \partial V^+ \quad (9)$$

$$-\vec{E}^{inc}\left(\vec{r}\right) = -j\omega\mu_0\mathbf{L_0}\left(\vec{J}_s\right) - \mathbf{K_0^+}\left(\vec{M}_s\right), \vec{r} \in \partial V^- \quad (10)$$

$$-\vec{H}^{inc}\left(\vec{r}\right) = -j\omega\varepsilon_0\mathbf{L_0}\left(\vec{M}_s\right) + \mathbf{K_0^+}\left(\vec{J}_s\right), \vec{r} \in \partial V^- \quad (11)$$

in which $\mathbf{L_0}$ is a linear operator given in (3), and $\mathbf{K_0^\pm}$ is also a linear operator formulated as:

$$\begin{aligned}\mathbf{K_0^\pm}\left(\vec{X}\right) &= \pm\frac{\hat{n}}{2} \times \vec{X}\left(\vec{r}\right) \\ &+ P.V. \int_\Omega \nabla G_0\left(\vec{r}, \vec{r}'\right) \times \vec{X}\left(\vec{r}'\right) d\Omega'\end{aligned} \quad (12)$$

where $\hat{n}$ represents the outward unit normal vector of ∂V_d, and the $P.V.$ represents the Cauchy principal value of the integration. The $\vec{J}_s$ and $\vec{M}_s$ are related to the total field on the ∂V_d:

$$\begin{cases}\vec{J}_s = \hat{n} \times \vec{H}^{tot} \\ \vec{M}_s = \vec{E}^{tot} \times \hat{n}\end{cases} \quad (13)$$

Equation (13) can be verified by $\hat{n} \times [(8) - (10)]$ and $\hat{n} \times [(9) - (11)]$.

In the second subproblem, the total field outside the dielectric body is assumed to be zero, while the total field inside the dielectric body remains unchanged, as shown in Fig. 2b. Note that the excitation sources which produce the incident field could be removed, and the media parameters of V_0 can be replaced with (ϵ_d, μ_0) in this subproblem according to the surface equivalence principle. Therefore the whole space becomes an infinite homogeneous space with media parameters (ϵ_d, μ_0) [19]. In this problem, also there are equivalent electric and magnetic currents on the surface of the dielectric body. Besides, these surface equivalent currents in this interior equivalent problem have equal amplitudes but opposite directions compared with those of external equivalent problem, as shown in Fig. 2. The surface equivalence principle indicates that the equivalent electric and magnetic currents generate zero field outside the dielectric body and total field inside the dielectric body. Therefore, the following four SIEs can be acquired:

$$0 = -j\omega\mu_0\mathbf{L_d}\left(-\vec{J}_s\right) - \mathbf{K_d^-}\left(-\vec{M}_s\right), \vec{r} \in \partial V^+ \quad (14)$$

$$0 = -j\omega\varepsilon_d \mathbf{L_d}\left(-\vec{M}_s\right) + \mathbf{K_d^-}\left(-\vec{J}_s\right), \vec{r} \in \partial V^+ \tag{15}$$

$$\vec{E}^{tot}(\vec{r}) = -j\omega\mu_0 \mathbf{L_d}\left(-\vec{J}_s\right) - \mathbf{K_d^+}\left(-\vec{M}_s\right), \vec{r} \in \partial V^- \tag{16}$$

$$\vec{H}^{tot}(\vec{r}) = -j\omega\varepsilon_d \mathbf{L_d}\left(-\vec{M}_s\right) + \mathbf{K_d^+}\left(-\vec{J}_s\right), \vec{r} \in \partial V^- \tag{17}$$

in which $\mathbf{L_d}$ and $\mathbf{K_d^\pm}$ are linear operators similar to $\mathbf{L_0}$ and $\mathbf{K_0^\pm}$ but replace the wave number and Green's function in background media with those of dielectric region.

By applying the surface equivalence principle, we have obtained eight SIEs, i.e., (8) - (11) and (14) - (17). In the following, we will illustrate how to derive all existing SIE-based CM formulations using the eight SIEs.

1) Formulation in [6]

The first approach to solve the CMs of dielectric bodies using SIE is presented in [6]. Subtracting (8) from (16), we obtain

$$j\omega\mu_0\left[\mathbf{L_d} + \mathbf{L_0}\right]\left(\vec{J}_s\right) + \left[\mathbf{K_d^+} + \mathbf{K_0^-}\right]\left(\vec{M}_s\right) = \vec{E}^{inc} \tag{18}$$

Similarly, subtracting (9) from (17), we have

$$-\left[\mathbf{K_d^+} + \mathbf{K_0^-}\right]\left(\vec{J}_s\right) + j\omega\left[\varepsilon_d\mathbf{L_d} + \varepsilon_0\mathbf{L_0}\right]\left(\vec{M}_s\right) = \vec{H}^{inc} \tag{19}$$

Combining (18) and (19), and rewriting them in a matrix form as follows

$$\begin{bmatrix} j\omega\mu_0\left(\mathbf{L_d} + \mathbf{L_0}\right) & \mathbf{K_d^+} + \mathbf{K_0^-} \\ -\left(\mathbf{K_d^+} + \mathbf{K_0^-}\right) & j\omega\left(\varepsilon_d\mathbf{L_d} + \varepsilon_0\mathbf{L_0}\right) \end{bmatrix} \cdot \begin{bmatrix} \vec{J}_s \\ \vec{M}_s \end{bmatrix} = \begin{bmatrix} \vec{E}^{inc} \\ \vec{H}^{inc} \end{bmatrix} \tag{20}$$

To ensure that the impedance matrix is symmetric, it is convenient to rearrange (20) into the form

$$\mathbf{Z}_{[6]} \cdot \begin{bmatrix} \vec{J}_s \\ j\vec{M}_s \end{bmatrix} = \begin{bmatrix} \vec{E}^{inc} \\ j\vec{H}^{inc} \end{bmatrix} \tag{21}$$

in which

$$\mathbf{Z}_{[6]} = \begin{bmatrix} j\omega\mu_0\left(\mathbf{L_d} + \mathbf{L_0}\right) & -j\left(\mathbf{K_d^+} + \mathbf{K_0^-}\right) \\ -j\left(\mathbf{K_d^+} + \mathbf{K_0^-}\right) & j\omega\left(\varepsilon_d\mathbf{L_d} + \varepsilon_0\mathbf{L_0}\right) \end{bmatrix} \tag{22}$$

Then the CMs are solved by the same way as (6) and (7). Note that the impedance matrix $\mathbf{Z}$ in (7) should be replaced with $\mathbf{Z}_{[6]}$ in (22). The subscript of $\mathbf{Z}_{[6]}$ refers to the index of the corresponding reference to distinguish from others impedance matrix, and the same goes for subsequent sections.

2) Formulations in [8], [9]

It is observed that the approach of [6] resulted in spurious modes [7]. To fix this problem, two single-source formulations are briefly reported in which the equivalent electric or magnetic current is alternatively involved [8]. Subsequently, the formulations of [8] are elaborated in [9]. The formulations of [8], [9] are based on (18) and (19). Firstly, it is assumed that $\vec{H}^{inc} = 0$ in (19), thus $\vec{M}_s$ can be expressed in terms of $\vec{J}_s$

$$\vec{M}_s = \left[j\omega\left(\varepsilon_d\mathbf{L_d} + \varepsilon_0\mathbf{L_0}\right)\right]^{-1}\left(\mathbf{K_d^+} + \mathbf{K_0^-}\right)\left(\vec{J}_s\right) \tag{23}$$

Then substituting (23) into (18), a single-source formulation is obtained

$$j\omega\mu_0\left[\mathbf{L_d} + \mathbf{L_0}\right]\left(\vec{J}_s\right) + \left[\mathbf{K_d^+} + \mathbf{K_0^-}\right]\left(\vec{M}_s\right) = \mathbf{Z}_{[9]}^{\mathbf{J}} \cdot \vec{J}_s \tag{24}$$

in which

$$\mathbf{Z}_{[9]}^{\mathbf{J}} = j\omega\mu_0\left(\mathbf{L_d} + \mathbf{L_0}\right) + \left(\mathbf{K_d^+} + \mathbf{K_0^-}\right)\left[j\omega\left(\varepsilon_d\mathbf{L_d} + \varepsilon_0\mathbf{L_0}\right)\right]^{-1}\left(\mathbf{K_d^+} + \mathbf{K_0^-}\right) \tag{25}$$

The superscript $\mathbf{J}$ indicates that the SIE only involves the electric current. Finally, the CMs are obtained using the similar approach as (6) and (7). Note that the impedance matrix $\mathbf{Z}$ in (7) should be replaced with $\mathbf{Z}_{[9]}^{\mathbf{J}}$ in (25).

Alternatively, we assume that $\vec{E}^{inc} = 0$ in (18), thus $\vec{J}_s$ can be expressed in terms of $\vec{M}_s$

$$\vec{J}_s = -\left[j\omega\mu_0\left(\mathbf{L_d} + \mathbf{L_0}\right)\right]^{-1}\left(\mathbf{K_d^+} + \mathbf{K_0^-}\right)\left(\vec{M}_s\right) \tag{26}$$

Substituting (26) into (19), another single-source formulation is acquired

$$-\left[\mathbf{K_d^+} + \mathbf{K_0^-}\right]\left(\vec{J}_s\right) + j\omega\left[\varepsilon_d\mathbf{L_d} + \varepsilon_0\mathbf{L_0}\right]\left(\vec{M}_s\right) = \mathbf{Z}_{[9]}^{\mathbf{M}} \cdot \vec{M}_s \tag{27}$$

where

$$\mathbf{Z}_{[9]}^{\mathbf{M}} = j\omega\left(\varepsilon_d\mathbf{L_d} + \varepsilon_0\mathbf{L_0}\right) + \left(\mathbf{K_d^+} + \mathbf{K_0^-}\right)\left[j\omega\mu_0\left(\mathbf{L_d} + \mathbf{L_0}\right)\right]^{-1}\left(\mathbf{K_d^+} + \mathbf{K_0^-}\right) \tag{28}$$

Also the CMs are solved using (6) and (7) but replace the impedance matrix $\mathbf{Z}$ in (7) with $\mathbf{Z}_{[9]}^{\mathbf{M}}$ in (28).

3) Formulations in [10]

Five types of SIE-based TCM formulations are presented in [10]. These five types formulations are derived in a unified manner. Three formulations lead to the same generalized eigenvalue equations as in [6], [9], while other two formulations result in two new generalized eigenvalue equations. The two proposed formulations which determine the CMs are [10]

$$\mathbf{Z}_{[10]}^{\mathbf{J}} = j\omega\mu_0\left(\mathbf{L_d} + \mathbf{L_0}\right) + \mathbf{K_d^+} \cdot \left(j\omega\varepsilon_d\mathbf{L_d}\right)^{-1} \cdot \mathbf{K_d^-} + \mathbf{K_0^-} \cdot \left(j\omega\varepsilon_0\mathbf{L_0}\right)^{-1} \cdot \mathbf{K_0^+} \tag{29}$$

$$\mathbf{Z}_{[10]}^{\mathbf{M}} = j\omega\left(\varepsilon_d\mathbf{L_d} + \varepsilon_0\mathbf{L_0}\right) + \mathbf{K_d^+} \cdot \left(j\omega\mu_0\mathbf{L_d}\right)^{-1} \cdot \mathbf{K_d^-} + \mathbf{K_0^-} \cdot \left(j\omega\mu_0\mathbf{L_0}\right)^{-1} \cdot \mathbf{K_0^+} \tag{30}$$

The CMs are solved using the similar approach as (6) and (7) but replace the impedance matrix $\mathbf{Z}$ in (7) with $\mathbf{Z}_{[10]}^{\mathbf{J}}$ and $\mathbf{Z}_{[10]}^{\mathbf{M}}$.

4) Formulations in [11]

Also adopting the current elimination method, two alternative formulations are presented in [11]. The major advantage of formulations in [11] is that no restriction is imposed on incident fields. As observed from (23) and (26), $\vec{H}^{inc} = 0$ or $\vec{E}^{inc} = 0$ is assumed to derive the dependence relationships between $\vec{J}_s$ and $\vec{M}_s$. For the CM formulations in [11], the dependence relationships between $\vec{J}_s$ and $\vec{M}_s$ are directly derived using (14) and (15), where neither $\vec{H}^{inc} = 0$ nor $\vec{E}^{inc} = 0$ is required.

According to (14), $\vec{J}_s$ can be obtained using $\vec{M}_s$ without considering the incident fields

$$\vec{J}_s = \mathbf{T_{MJ}} \cdot \vec{M}_s \tag{31}$$

in which

$$\mathbf{T_{MJ}} = -(j\omega\mu_0\mathbf{L_d})^{-1} \cdot \mathbf{K_d^-} \tag{32}$$

Substituting (31) into (21), we have

$$\mathbf{Z}_{[6]} \cdot \begin{bmatrix} \mathbf{T_{MJ}} \\ j\mathbf{I} \end{bmatrix} \cdot \vec{M}_s = \begin{bmatrix} \vec{E}^{inc} \\ j\vec{H}^{inc} \end{bmatrix} \tag{33}$$

where $\mathbf{I}$ refers to the identity operator. Then both sides of (33) multiply by $\begin{bmatrix} \mathbf{T_{MJ}}^H & (j\mathbf{I})^H \end{bmatrix}$ results in

$$\mathbf{Z}^{\mathbf{M}}_{[\mathbf{11}]} \cdot \vec{M}_s = \begin{bmatrix} \mathbf{T_{MJ}}^H & (j\mathbf{I})^H \end{bmatrix} \cdot \begin{bmatrix} \vec{E}^{inc} \\ j\vec{H}^{inc} \end{bmatrix} \tag{34}$$

in which

$$\mathbf{Z}^{\mathbf{M}}_{[\mathbf{11}]} = \begin{bmatrix} \mathbf{T_{MJ}}^H & (j\mathbf{I})^H \end{bmatrix} \cdot \mathbf{Z}_{[6]} \cdot \begin{bmatrix} \mathbf{T_{MJ}} \\ j\mathbf{I} \end{bmatrix} \tag{35}$$

The well-designed operator $\begin{bmatrix} \mathbf{T_{MJ}}^H & (j\mathbf{I})^H \end{bmatrix}$ on the left-hand side of $\mathbf{Z}_{[6]}$ and its conjugate transpose operator on the right-hand side of $\mathbf{Z}_{[6]}$ express $\vec{J}_s$ in terms of $\vec{M}_s$ to ensure that the resulted eigenvalues have reasonable physical meanings related to electromagnetic powers [11].

Alternatively, $\vec{M}_s$ can be acquired using $\vec{J}_s$ according to (15) without considering specific incident fields, and the following single-source SIE in which only $\vec{J}_s$ is involved could be derived

$$\mathbf{Z}^{\mathbf{J}}_{[\mathbf{11}]} \cdot \vec{J}_s = \begin{bmatrix} \mathbf{I}^H & (j\mathbf{T_{JM}})^H \end{bmatrix} \cdot \begin{bmatrix} \vec{E}^{inc} \\ j\vec{H}^{inc} \end{bmatrix} \tag{36}$$

where

$$\mathbf{Z}^{\mathbf{J}}_{[\mathbf{11}]} = \begin{bmatrix} \mathbf{I}^H & (j\mathbf{T_{JM}})^H \end{bmatrix} \cdot \mathbf{Z}_{[6]} \cdot \begin{bmatrix} \mathbf{I} \\ j\mathbf{T_{JM}} \end{bmatrix} \tag{37}$$

$$\mathbf{T_{JM}} = (j\omega\varepsilon_d\mathbf{L_d})^{-1} \cdot \mathbf{K_d^-} \tag{38}$$

Finally, the CMs are calculated using (6) and (7) but replace the impedance matrix $\mathbf{Z}$ in (7) with $\mathbf{Z}^{\mathbf{M}}_{[\mathbf{11}]}$ and $\mathbf{Z}^{\mathbf{J}}_{[\mathbf{11}]}$.

5) Formulations in [12]

Applying the current elimination method, two novel formulations are proposed in [12]. Differently from the formulations described above, the CMs are solved by two special generalized eigenvalue equations [12].

Firstly, it is assumed that $\vec{E}^{inc} = 0$ in (10), we have

$$j\omega\mu_0\mathbf{L_0}\left(\vec{J}_s\right) + \mathbf{K_0^+}\left(\vec{M}_s\right) = 0 \tag{39}$$

Using (15), $\vec{M}_s$ can be expressed in terms of $\vec{J}_s$

$$\vec{M}_s = \mathbf{T_{JM}} \cdot \vec{J}_s \tag{40}$$

in which $\mathbf{T_{JM}}$ is identical to (38). Substituting (40) into (39) results in

$$\mathbf{Z}^{\mathbf{J}}_{[\mathbf{12}]} \cdot \vec{J}_s = 0 \tag{41}$$

where

$$\mathbf{Z}^{\mathbf{J}}_{[\mathbf{12}]} = j\omega\mu_0\mathbf{L_0} + \mathbf{K_0^+} \cdot (j\omega\varepsilon_d\mathbf{L_d})^{-1} \cdot \mathbf{K_d^-} \tag{42}$$

Alternatively, we assume $\vec{H}^{inc} = 0$ in (11), we have

$$j\omega\varepsilon_0\mathbf{L_0}\left(\vec{M}_s\right) - \mathbf{K_0^+}\left(\vec{J}_s\right) = 0 \tag{43}$$

Using (14), $\vec{J}_s$ can be expressed in terms of $\vec{M}_s$ as $\vec{J}_s = \mathbf{T_{MJ}} \cdot \vec{M}_s$ where $\mathbf{T_{MJ}}$ is given by (32). Applying the current elimination method to (43), we have

$$\mathbf{Z}^{\mathbf{M}}_{[\mathbf{12}]} \cdot \vec{M}_s = 0 \tag{44}$$

in which

$$\mathbf{Z}^{\mathbf{M}}_{[\mathbf{12}]} = j\omega\varepsilon_0\mathbf{L_0} + \mathbf{K_0^+} \cdot (j\omega\mu_0\mathbf{L_d})^{-1} \cdot \mathbf{K_d^-} \tag{45}$$

Finally, the CMs are solved by the following generalized eigenvalue equations

$$\mathbf{Z}^{\mathbf{J}}_{[\mathbf{12}]} \cdot \vec{J}_n = (1 + j\lambda_n)\,\mathbf{R}^{\mathbf{J}}_{[\mathbf{12}]} \cdot \vec{J}_n \tag{46}$$

$$\mathbf{Z}^{\mathbf{M}}_{[\mathbf{12}]} \cdot \vec{M}_n = (1 + j\lambda_n)\,\mathbf{R}^{\mathbf{M}}_{[\mathbf{12}]} \cdot \vec{M}_n \tag{47}$$

in which $\mathbf{R}^{\mathbf{J}}_{[\mathbf{12}]}$ and $\mathbf{R}^{\mathbf{M}}_{[\mathbf{12}]}$ are well-designed operators related to the radiated power

$$\mathbf{R}^{\mathbf{J}}_{[\mathbf{12}]} = real\left\{j\omega\mu_0\mathbf{L_0}\right\} + j \cdot imag\left\{\mathbf{K_0^+}\right\} \cdot (j\omega\varepsilon_d\mathbf{L_d})^{-1} \cdot \mathbf{K_d^-} \tag{48}$$

$$\mathbf{R}^{\mathbf{M}}_{[\mathbf{12}]} = real\left\{j\omega\varepsilon_0\mathbf{L_0}\right\} + j \cdot imag\left\{\mathbf{K_0^+}\right\} \cdot (j\omega\mu_0\mathbf{L_d})^{-1} \cdot \mathbf{K_d^-} \tag{49}$$

where $real\{\cdot\}$ and $imag\{\cdot\}$ represent the real and imaginary part, respectively. The inspiration to construct $\mathbf{R}^{\mathbf{J}}_{[\mathbf{12}]}$ and $\mathbf{R}^{\mathbf{M}}_{[\mathbf{12}]}$ related to the radiated power comes from the combined field integral equation-based TCM [22]. Note that the formulations of current elimination in [12] are same with those of [11]. The difference between the CMs formulations in [11] and [12] is how to construct the generalized eigenvalue equations.

6) Formulation in [13]

Recently, it is found that the current elimination process can be avoided by properly selecting the weighting operator of the generalized eigenvalue equation in terms of the integral operators related to the background media [13]. The CMs can be directly solved by the following eigenvalue equation

$$\mathbf{Z}_{[6]} \cdot \begin{bmatrix} \vec{J}_n \\ j\vec{M}_n \end{bmatrix} = (1 + j\lambda_n)\,\mathbf{R}_{[\mathbf{13}]} \cdot \begin{bmatrix} \vec{J}_n \\ j\vec{M}_n \end{bmatrix} \tag{50}$$

in which $\mathbf{Z}_{[6]}$ is identical to (22), and $\mathbf{R}_{[\mathbf{13}]}$ is a weighting operator in terms of the real and imaginary parts of the integral operators only related to the background media

$$\mathbf{R}_{[\mathbf{13}]} = \begin{bmatrix} real\left\{j\omega\mu_0\mathbf{L_0}\right\} & imag\left\{\mathbf{K_0^-}\right\} \\ imag\left\{\mathbf{K_0^-}\right\} & real\left\{j\omega\varepsilon_0\mathbf{L_0}\right\} \end{bmatrix} \tag{51}$$

III. IMPLEMENTATION OF THE EXISTING SIE-BASED TCM FORMULATIONS

Since there are so many different formulations to calculate the CMs of dielectric bodies, it would be interesting to make a comprehensive comparison among them. We summarize the existing computation formulations in Table 1 for comparison. More importantly, the computation results of these formulations should be compared to make the relationship and distinction among these formulations clear. We must implement all of the existing SIE-based TCM formulations to obtain the computation results of them. In this section, we present a procedure to implement all of the existing SIE-based TCM formulations in a unified manner.

It can be observed from Table 1 that the operators related to the calculations of the CMs are combinations of six basic operators, i.e., $\mathbf{L_0}$, $\mathbf{L_d}$, $\mathbf{K_0^+}$, $\mathbf{K_0^-}$, $\mathbf{K_d^+}$, and $\mathbf{K_d^-}$. Applying the method of moments (MoM) [23] with Galerkin testing procedure, these operators can be transformed into matrices as

$$\begin{aligned}[\mathbf{L_i}]_{mn} = &\int\limits_{\Omega_m} \vec{f}_m(\vec{r}) \cdot \int\limits_{\Omega_n} \vec{f}_n\left(\vec{r}'\right) G_i d\Omega_n d\Omega_m \\ &- \frac{1}{k_i^2}\int\limits_{\Omega_m} \nabla\cdot\vec{f}_m(\vec{r}) \int\limits_{\Omega_n} \nabla'\cdot\vec{f}_n\left(\vec{r}'\right) G_i d\Omega_n d\Omega_m\end{aligned} \tag{52}$$

$$\left[\mathbf{K_i^{PV}}\right]_{mn} = P.V.\int\limits_{\Omega_m} \vec{f}_m(\vec{r}) \cdot \int\limits_{\Omega_n} \nabla G_i \times \vec{f}_n\left(\vec{r}'\right) d\Omega_n d\Omega_m \tag{53}$$

$$[\mathbf{K}]_{mn} = \int\limits_{\Omega_m} \vec{f}_m(\vec{r}) \cdot \left[\frac{\hat{n}}{2} \times \vec{f}_n(\vec{r})\right] d\Omega_m \tag{54}$$

$$\left[\mathbf{K_i^{\pm}}\right]_{mn} = \left[\mathbf{K_i^{PV}}\right]_{mn} \pm [\mathbf{K}]_{mn} \tag{55}$$

in which $i = 0$ or d. The $\vec{f}_m$ and $\vec{f}_n$ represent the mth testing function and the nth basis function, respectively. The basis function and testing function both are RWG function [24] in this paper. The Ω_m and Ω_n denote the regions occupied by the $\vec{f}_m$ and $\vec{f}_n$, respectively. The $[\cdot]_{mn}$ represents the element located in the mth row and the nth column of corresponding matrix. As can be observed, only five basic matrices need to be calculated, i.e., $\mathbf{L_0}$, $\mathbf{L_d}$, $\mathbf{K_0^{PV}}$, $\mathbf{K_d^{PV}}$, and $\mathbf{K}$. Once we have obtained above submatrices, all of the matrices related to the existing SIE-based TCM formulations can be assembled by these submatrices according to Table 1 without repeating computations. It will save a lot of time to calculate the results of the existing SIE-based TCM formulations.

IV. CROSS-VALIDATION OF EXISTING FORMULATIONS

In this section, we use the method described above to calculate the CMs of a lossless dielectric cylinder of radius 5.25 mm, height 4.6 mm, and $\epsilon_r = 38, \mu_r = 1$. The frequency band is from 4.5 GHz to 8 GHz with 50 MHz interval. Although the case has often been used to verify the results of CMs formulations [9]–[12], a complete comparison between the existing CMs formulations has not been found. We herein present a complete comparison of all CMs formulations, and they are cross-validated by the numerical results. All computations have been carried out with in-house MATLAB codes using a workstation computer with Intel(R) Xeon (R) X5650 CPU 2.67 GHz and 64 GB RAM.

The modal significance (MS) is an intrinsic parameter of CMs that indicates whether the mode is resonant. The MS is defined by $MS_n = \left|\frac{1}{1+j\lambda_n}\right|$. The MS transforms the $[-\infty, +\infty]$ range of λ_n into a much smaller range of $[0, 1]$, thus the MS is more convenient than λ_n to investigate the resonant behaviors over a wide frequency band. The modes with MS approach to 1 are resonant. Figure 3 depicts the MS curves of the first 100 modes obtained from the existing CMs formulations within the frequency band 4.5 GHz to 8 GHz. The resonant frequencies can be found by locating the maximal values of MS curves. There are many degenerate modes owing to the symmetry of the cylinder. In Fig. 3, we label the resonant frequency and degeneracy (inside of the parenthesis). It was reported that there were eight resonant modes (including degenerate modes) within the frequency band 4.5 GHz to 8 GHz, i.e., TE_{01}, HEM_{11}, HEM_{12}, TM_{01}, and HEM_{21} [25]. Note that the HEM modes are degenerate. For convenience, we list the resonant frequency and degeneracy (inside of the parenthesis) obtained from different methods in Table 2. It can be observed from Table 2 that all existing CMs formulations give the reasonable resonant frequencies and degeneracies of resonant modes within the frequency band 4.5 GHz to 8 GHz, compared with the result of eigenmodes in [26] and measurement result of [27]. Furthermore, we investigate the electric fields, magnetic fields, and radiation patterns of the resonant modes obtained from all existing CMs formulations. We found that the fields and radiation patterns of the resonant modes obtained from different methods are almost identical, which are depicted in Fig. 4 to 6.

However, some noticeable relationships among the results obtained from these methods could be found if we carefully compare these MS curves:

1) The VIE-based TCM in [5] and the SIE-based TCM in [11]–[13] give very similar MS curves for not only the aforementioned eight resonant modes but also the higher-order modes which are not resonant within the frequency band. Note that the MS of HEM_{21} modes at 7.8 GHz obtained from the VIE-based TCM is closer to 1 than those of the SIE-based TCM. It is caused by the numerical errors of different methods and does not affect the resonant frequencies. It indicates that these different approaches may lead to identical modal solutions. Some mathematical proof had been presented in [11]. It is proved rigorously that the SIE-based TCM of [11] and the VIE-based TCM of [5] result in identical modal results. Other mathematical proof of the connection between the VIE-based TCM and the SIE-based TCM need the efforts of CMs community and beyond of the scope of this paper.

This article has been accepted for publication in a future issue of this journal, but has not been fully edited. Content may change prior to final publication. Citation information: DOI 10.1109/ACCESS.2019.2963278, IEEE Access

TABLE 1: Summary of existing IE-based TCM formulations

Methods	Generalized eigenvalue equations	Related operators
VIE-based CM in [5]	$\mathbf{X}\cdot\vec{J}_n=\lambda_n\mathbf{R}\cdot\vec{J}_n$	$\mathbf{Z}=j\omega\mathbf{L_0}+(j\omega\Delta\varepsilon)^{-1}\cdot\mathbf{I}$ $\mathbf{R}=\frac{1}{2}\left(\mathbf{Z}+\mathbf{Z}^H\right),\mathbf{X}=\frac{1}{2j}\left(\mathbf{Z}-\mathbf{Z}^H\right)$
Formulation in [6]	$\mathbf{X}\cdot\begin{bmatrix}\vec{J}_n\\ j\vec{M}_n\end{bmatrix}=\lambda_n\mathbf{R}\cdot\begin{bmatrix}\vec{J}_n\\ j\vec{M}_n\end{bmatrix}$	$\mathbf{Z}_{[6]}=\begin{bmatrix}j\omega\mu_0\left(\mathbf{L_d}+\mathbf{L_0}\right) & -j\left(\mathbf{K_d^+}+\mathbf{K_0^-}\right)\\ -j\left(\mathbf{K_d^+}+\mathbf{K_0^-}\right) & j\omega\left(\varepsilon_d\mathbf{L_d}+\varepsilon_0\mathbf{L_0}\right)\end{bmatrix}$ $\mathbf{R}=\frac{1}{2}\left(\mathbf{Z}_{[6]}+\mathbf{Z}_{[6]}{}^H\right),\mathbf{X}=\frac{1}{2j}\left(\mathbf{Z}_{[6]}-\mathbf{Z}_{[6]}{}^H\right)$
J-formulation in [8], [9]	$\mathbf{X}\cdot\vec{J}_n=\lambda_n\mathbf{R}\cdot\vec{J}_n$	$\mathbf{Z}_{[9]}^{\mathbf{J}}=j\omega\mu_0\left(\mathbf{L_d}+\mathbf{L_0}\right)$ $+\left(\mathbf{K_d^+}+\mathbf{K_0^-}\right)\left[j\omega\left(\varepsilon_d\mathbf{L_d}+\varepsilon_0\mathbf{L_0}\right)\right]^{-1}\left(\mathbf{K_d^+}+\mathbf{K_0^-}\right)$ $\mathbf{R}=\frac{1}{2}\left[\mathbf{Z}_{[9]}^{\mathbf{J}}+\left(\mathbf{Z}_{[9]}^{\mathbf{J}}\right)^H\right],\mathbf{X}=\frac{1}{2j}\left[\mathbf{Z}_{[9]}^{\mathbf{J}}-\left(\mathbf{Z}_{[9]}^{\mathbf{J}}\right)^H\right]$
M-formulation in [8], [9]	$\mathbf{X}\cdot\vec{M}_n=\lambda_n\mathbf{R}\cdot\vec{M}_n$	$\mathbf{Z}_{[9]}^{\mathbf{M}}=j\omega\left(\varepsilon_d\mathbf{L_d}+\varepsilon_0\mathbf{L_0}\right)$ $+\left(\mathbf{K_d^+}+\mathbf{K_0^-}\right)\left[j\omega\mu_0\left(\mathbf{L_d}+\mathbf{L_0}\right)\right]^{-1}\left(\mathbf{K_d^+}+\mathbf{K_0^-}\right)$ $\mathbf{R}=\frac{1}{2}\left[\mathbf{Z}_{[9]}^{\mathbf{M}}+\left(\mathbf{Z}_{[9]}^{\mathbf{M}}\right)^H\right],\mathbf{X}=\frac{1}{2j}\left[\mathbf{Z}_{[9]}^{\mathbf{M}}-\left(\mathbf{Z}_{[9]}^{\mathbf{M}}\right)^H\right]$
J-formulation in [10]	$\mathbf{X}\cdot\vec{J}_n=\lambda_n\mathbf{R}\cdot\vec{J}_n$	$\mathbf{Z}_{[\mathbf{10}]}^{\mathbf{J}}=j\omega\mu_0\left(\mathbf{L_d}+\mathbf{L_0}\right)$ $+\mathbf{K_d^+}\cdot\left(j\omega\varepsilon_d\mathbf{L_d}\right)^{-1}\cdot\mathbf{K_d^-}+\mathbf{K_0^-}\cdot\left(j\omega\varepsilon_0\mathbf{L_0}\right)^{-1}\cdot\mathbf{K_0^+}$ $\mathbf{R}=\frac{1}{2}\left[\mathbf{Z}_{[\mathbf{10}]}^{\mathbf{J}}+\left(\mathbf{Z}_{[\mathbf{10}]}^{\mathbf{J}}\right)^H\right],\mathbf{X}=\frac{1}{2j}\left[\mathbf{Z}_{[\mathbf{10}]}^{\mathbf{J}}-\left(\mathbf{Z}_{[\mathbf{10}]}^{\mathbf{J}}\right)^H\right]$
M-formulation in [10]	$\mathbf{X}\cdot\vec{M}_n=\lambda_n\mathbf{R}\cdot\vec{M}_n$	$\mathbf{Z}_{[\mathbf{10}]}^{\mathbf{M}}=j\omega\left(\varepsilon_d\mathbf{L_d}+\varepsilon_0\mathbf{L_0}\right)$ $+\mathbf{K_d^+}\cdot\left(j\omega\mu_0\mathbf{L_d}\right)^{-1}\cdot\mathbf{K_d^-}+\mathbf{K_0^-}\cdot\left(j\omega\mu_0\mathbf{L_0}\right)^{-1}\cdot\mathbf{K_0^+}$ $\mathbf{R}=\frac{1}{2}\left[\mathbf{Z}_{[\mathbf{10}]}^{\mathbf{M}}+\left(\mathbf{Z}_{[\mathbf{10}]}^{\mathbf{M}}\right)^H\right],\mathbf{X}=\frac{1}{2j}\left[\mathbf{Z}_{[\mathbf{10}]}^{\mathbf{M}}-\left(\mathbf{Z}_{[\mathbf{10}]}^{\mathbf{M}}\right)^H\right]$
J-formulation in [11]	$\mathbf{X}\cdot\vec{J}_n=\lambda_n\mathbf{R}\cdot\vec{J}_n$	$\mathbf{Z}_{[\mathbf{11}]}^{\mathbf{J}}=\begin{bmatrix}\mathbf{I}^H & \left(j\mathbf{T_{JM}}\right)^H\end{bmatrix}\cdot\mathbf{Z}_{[6]}\cdot\begin{bmatrix}\mathbf{I}\\ j\mathbf{T_{JM}}\end{bmatrix}$ $\mathbf{T_{JM}}=\left(j\omega\varepsilon_d\mathbf{L_d}\right)^{-1}\cdot\mathbf{K_d^-}$ $\mathbf{R}=\frac{1}{2}\left[\mathbf{Z}_{[\mathbf{11}]}^{\mathbf{J}}+\left(\mathbf{Z}_{[\mathbf{11}]}^{\mathbf{J}}\right)^H\right],\mathbf{X}=\frac{1}{2j}\left[\mathbf{Z}_{[\mathbf{11}]}^{\mathbf{J}}-\left(\mathbf{Z}_{[\mathbf{11}]}^{\mathbf{J}}\right)^H\right]$
M-formulation in [11]	$\mathbf{X}\cdot\vec{M}_n=\lambda_n\mathbf{R}\cdot\vec{M}_n$	$\mathbf{Z}_{[\mathbf{11}]}^{\mathbf{M}}=\begin{bmatrix}\mathbf{T_{MJ}}^H & \left(j\mathbf{I}\right)^H\end{bmatrix}\cdot\mathbf{Z}_{[6]}\cdot\begin{bmatrix}\mathbf{T_{MJ}}\\ j\mathbf{I}\end{bmatrix}$ $\mathbf{T_{MJ}}=-\left(j\omega\mu_0\mathbf{L_d}\right)^{-1}\cdot\mathbf{K_d^-}$ $\mathbf{R}=\frac{1}{2}\left[\mathbf{Z}_{[\mathbf{11}]}^{\mathbf{M}}+\left(\mathbf{Z}_{[\mathbf{11}]}^{\mathbf{M}}\right)^H\right],\mathbf{X}=\frac{1}{2j}\left[\mathbf{Z}_{[\mathbf{11}]}^{\mathbf{M}}-\left(\mathbf{Z}_{[\mathbf{11}]}^{\mathbf{M}}\right)^H\right]$
J-formulation in [12]	$\mathbf{Z}_{[\mathbf{12}]}^{\mathbf{J}}\cdot\vec{J}_n=\left(1+j\lambda_n\right)\mathbf{R}_{[\mathbf{12}]}^{\mathbf{J}}\cdot\vec{J}_n$	$\mathbf{Z}_{[\mathbf{12}]}^{\mathbf{J}}=j\omega\mu_0\mathbf{L_0}+\mathbf{K_0^+}\cdot\left(j\omega\varepsilon_d\mathbf{L_d}\right)^{-1}\cdot\mathbf{K_d^-}$ $\mathbf{R}_{[\mathbf{12}]}^{\mathbf{J}}=real\left\{j\omega\mu_0\mathbf{L_0}\right\}+j\cdot imag\left\{\mathbf{K_0^+}\right\}\cdot\left(j\omega\varepsilon_d\mathbf{L_d}\right)^{-1}\cdot\mathbf{K_d^-}$
M-formulation in [12]	$\mathbf{Z}_{[\mathbf{12}]}^{\mathbf{M}}\cdot\vec{M}_n=\left(1+j\lambda_n\right)\mathbf{R}_{[\mathbf{12}]}^{\mathbf{M}}\cdot\vec{M}_n$	$\mathbf{Z}_{[\mathbf{12}]}^{\mathbf{M}}=j\omega\varepsilon_0\mathbf{L_0}+\mathbf{K_0^+}\cdot\left(j\omega\mu_0\mathbf{L_d}\right)^{-1}\cdot\mathbf{K_d^-}$ $\mathbf{R}_{[\mathbf{12}]}^{\mathbf{M}}=real\left\{j\omega\varepsilon_0\mathbf{L_0}\right\}+j\cdot imag\left\{\mathbf{K_0^+}\right\}\cdot\left(j\omega\mu_0\mathbf{L_d}\right)^{-1}\cdot\mathbf{K_d^-}$
Formulation in [13]	$\mathbf{Z}_{[6]}\cdot\begin{bmatrix}\vec{J}_n\\ j\vec{M}_n\end{bmatrix}=\left(1+j\lambda_n\right)\mathbf{R}_{[\mathbf{13}]}\cdot\begin{bmatrix}\vec{J}_n\\ j\vec{M}_n\end{bmatrix}$	$\mathbf{R}_{[\mathbf{13}]}=\begin{bmatrix}real\left\{j\omega\mu_0\mathbf{L_0}\right\} & imag\left\{\mathbf{K_0^-}\right\}\\ imag\left\{\mathbf{K_0^-}\right\} & real\left\{j\omega\varepsilon_0\mathbf{L_0}\right\}\end{bmatrix}$

This article has been accepted for publication in a future issue of this journal, but has not been fully edited. Content may change prior to final publication. Citation information: DOI 10.1109/ACCESS.2019.2963278, IEEE Access

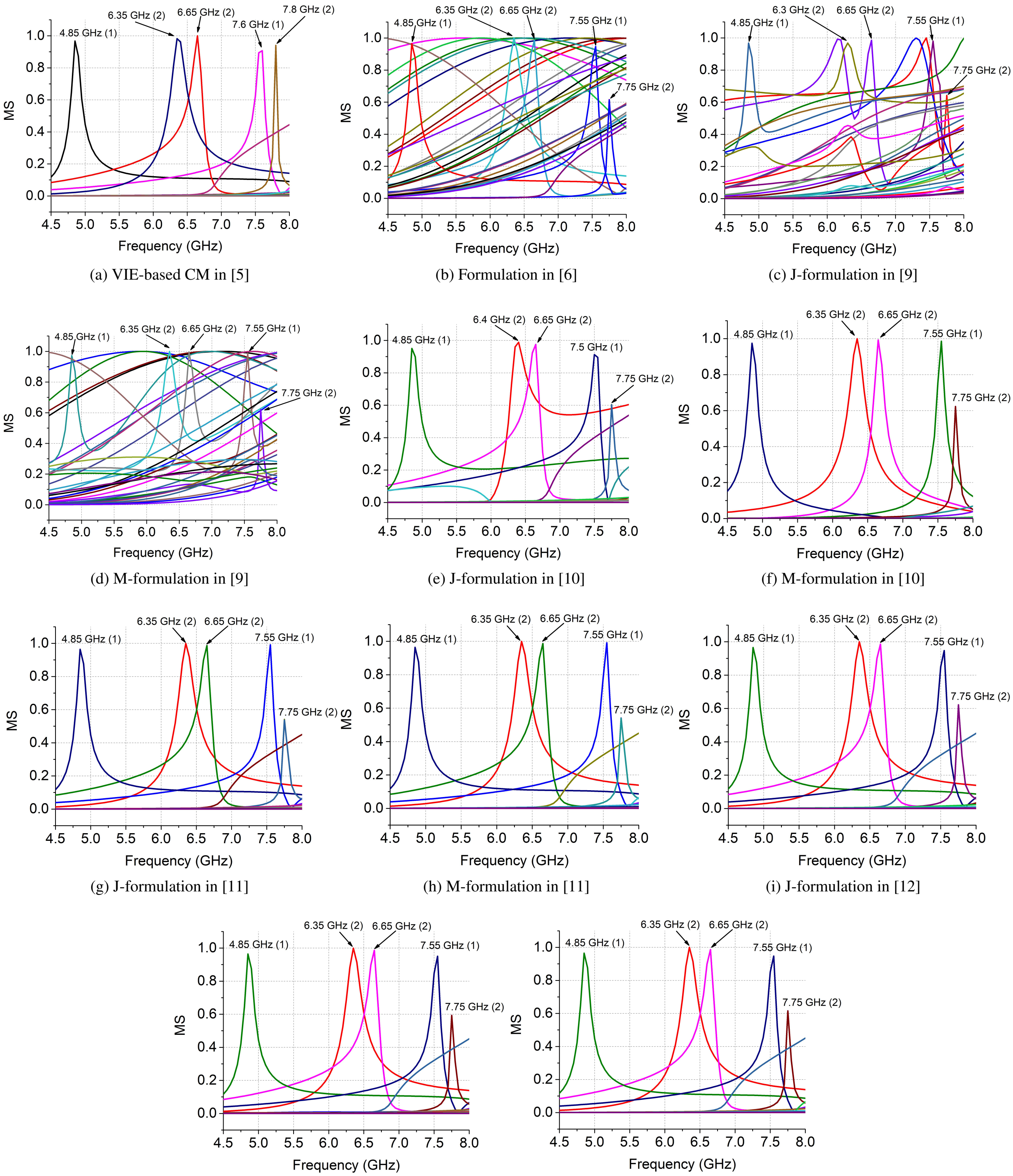

(a) VIE-based CM in [5]
(b) Formulation in [6]
(c) J-formulation in [9]
(d) M-formulation in [9]
(e) J-formulation in [10]
(f) M-formulation in [10]
(g) J-formulation in [11]
(h) M-formulation in [11]
(i) J-formulation in [12]
(j) M-formulation in [12]
(k) Formulation in [13]

FIGURE 3: The MS of first 100 modes obtained from the existing CMs formulations.

2) The result of the formulation in [6] contains many extra resonant modes, compared with the results of the approaches in [5], [11]–[13]. However, the MS curves of the aforementioned eight resonant modes are almost

This article has been accepted for publication in a future issue of this journal, but has not been fully edited. Content may change prior to final publication. Citation information: DOI 10.1109/ACCESS.2019.2963278, IEEE Access

TABLE 2: The resonant frequency and degeneracy (inside of the parenthesis) obtained from different methods

Method	TE_{01}	HEM_{11}	HEM_{12}	TM_{01}	HEM_{21}
Eigenmode [26]	4.83 GHz	6.33 GHz	6.63 GHz	7.52 GHz	7.75 GHz
Measurement result [27]	4.85 GHz	Null	6.64 GHz	7.6 GHz	7.81 GHz
VIE-based CM in [5]	4.85 GHz (1)	6.35 GHz (2)	6.65 GHz (2)	7.6 GHz (1)	7.8 GHz (2)
Formulation in [6]	4.85 GHz (1)	6.35 GHz (2)	6.65 GHz (2)	7.55 GHz (1)	7.75 GHz (1)
J-formulation in [9]	4.85 GHz (1)	6.3 GHz (2)	6.65 GHz (2)	7.55 GHz (1)	7.75 GHz (2)
M-formulation in [9]	4.85 GHz (1)	6.35 GHz (2)	6.65 GHz (2)	7.55 GHz (1)	7.75 GHz (2)
J-formulation in [10]	4.85 GHz (1)	6.4 GHz (2)	6.65 GHz (2)	7.5 GHz (1)	7.75 GHz (2)
M-formulation in [10]	4.85 GHz (1)	6.35 GHz (2)	6.65 GHz (2)	7.55 GHz (1)	7.75 GHz (1)
J-formulation in [11]	4.85 GHz (1)	6.35 GHz (2)	6.65 GHz (2)	7.55 GHz (1)	7.75 GHz (1)
M-formulation in [11]	4.85 GHz (1)	6.35 GHz (2)	6.65 GHz (2)	7.55 GHz (1)	7.75 GHz (1)
J-formulation in [12]	4.85 GHz (1)	6.35 GHz (2)	6.65 GHz (2)	7.55 GHz (1)	7.75 GHz (1)
M-formulation in [12]	4.85 GHz (1)	6.35 GHz (2)	6.65 GHz (2)	7.55 GHz (1)	7.75 GHz (1)
Formulation in [13]	4.85 GHz (1)	6.35 GHz (2)	6.65 GHz (2)	7.55 GHz (1)	7.75 GHz (1)

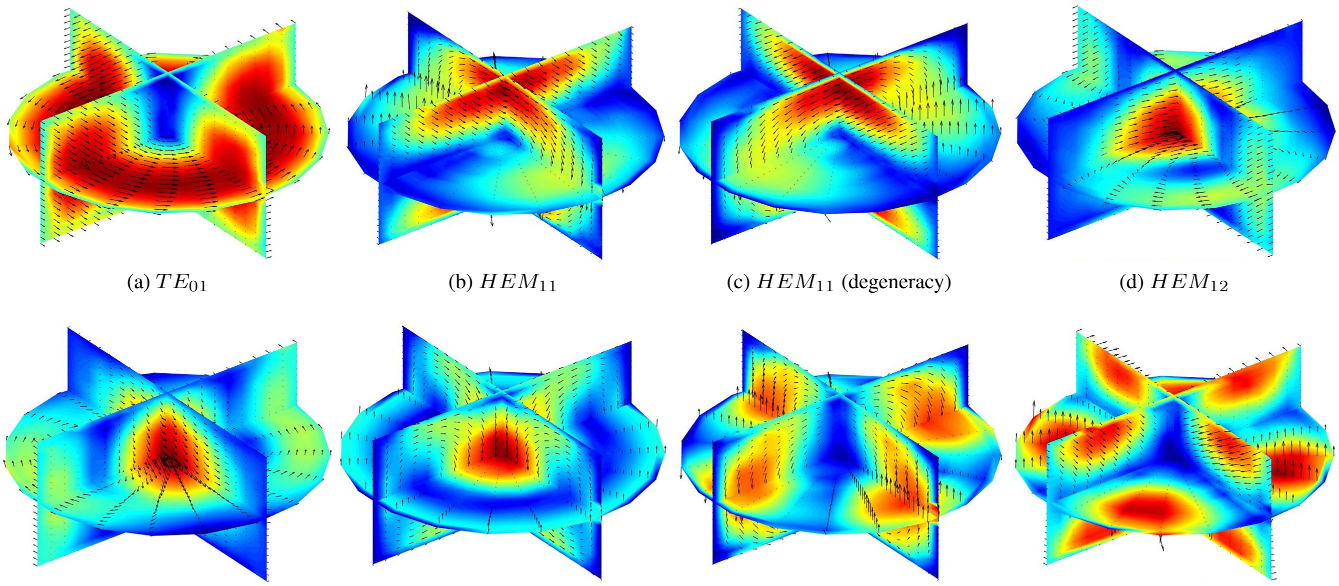

(a) TE_{01} (b) HEM_{11} (c) HEM_{11} (degeneracy) (d) HEM_{12}

(e) HEM_{12} (degeneracy) (f) TM_{01} (g) HEM_{21} (h) HEM_{21} (degeneracy)

FIGURE 4: Electric fields of resonant modes obtained from CMs formulations.

identical to those of [5], [11]–[13]. It indicates that the result of formulation in [6] not only could give several reasonable resonant modes but also bring some spurious modes.

3) The MS curves acquired from the J-formulation and M-formulation in [9] are quite different from those of [5], [11]–[13]. Besides, the MS curves indicate that there are more than eight resonant modes when considering the degenerate modes, which does not coincide with the results in [25]. In addition, the MS curves acquired from the J-formulation and M-formulation in [9] are not similar, as they should be. Therefore, there might be some problems on the formulations of [9].
4) The MS curves obtained from the J-formulation and M-formulation in [10] indicate five reasonable resonant frequencies and eight resonant modes. Besides, it seems that the results of formulations in [10] are immune from spurious modes. There are some minor differences between the MS curves of the J-formulation and M-formulation, as shown in Fig. 3e and 3f. Fortunately, the MS curves of J-formulation and M-formulation are still similar and provide reasonable resonant modes.

We also compare the computational efficiencies of different formulations. Table 3 lists the unknowns and computational time (in second) of all CMs formulations. The averaged mesh size of all computations equals one-tenth of the wavelength in the dielectric region at 8 GHz. The SWG basis function [28] is used for the VIE-based TCM formulation, and the RWG basis function [24] is employed for the SIE-based TCM formulations. The unknowns correspond to the numbers of SWG or RWG basis functions. The computational

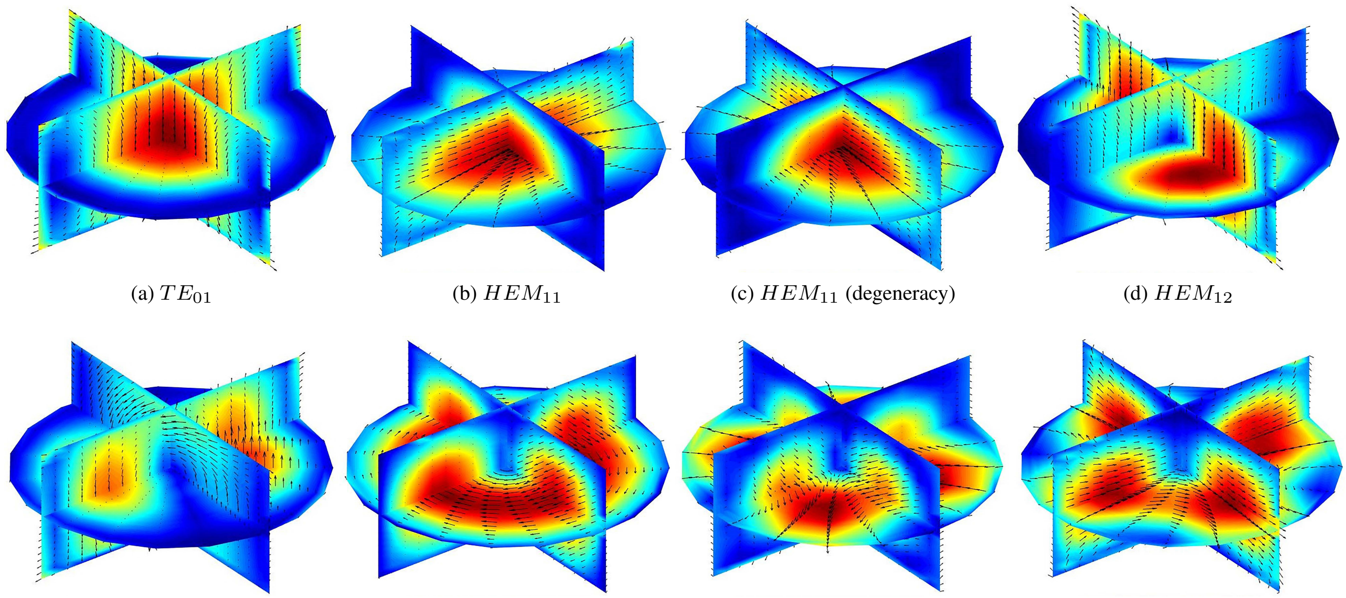

(a) TE_{01} (b) HEM_{11} (c) HEM_{11} (degeneracy) (d) HEM_{12}

(e) HEM_{12} (degeneracy) (f) TM_{01} (g) HEM_{21} (h) HEM_{21} (degeneracy)

FIGURE 5: Magnetic fields of resonant modes obtained from CMs formulations.

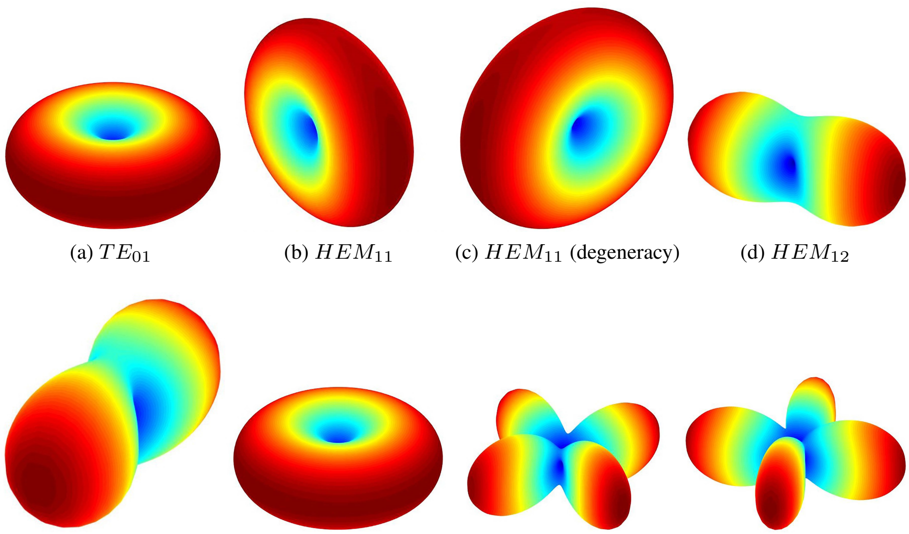

(a) TE_{01} (b) HEM_{11} (c) HEM_{11} (degeneracy) (d) HEM_{12}

(e) HEM_{12} (degeneracy) (f) TM_{01} (g) HEM_{21} (h) HEM_{21} (degeneracy)

FIGURE 6: Radiation patterns of resonant modes obtained from CMs formulations.

time includes the time for the computation of the impedance matrix and solving the generalized eigenvalue equation at a single frequency. It is obvious that the SIE-based TCM can greatly save the computational time, compared with the VIE-based TCM. This is the reason why much attention is paid for the SIE-based TCM. Besides, the computational time of the existing SIE-based TCM formulations is about the same level.

V. CONCLUSION

In this paper, we present an overview and a unified implementation procedure of the IE-based TCM formulations of dielectric bodies. The numerical results obtained using the existing TCM formulations for a dielectric body are also displayed and compared. We study the modal solutions of the first 100 modes of different methods to make a complete comparison. It is found that although all approaches could give the reasonable resonant modes, some of them bring extra modes. Besides, several different formulations result in

This article has been accepted for publication in a future issue of this journal, but has not been fully edited. Content may change prior to final publication. Citation information: DOI 10.1109/ACCESS.2019.2963278, IEEE Access

TABLE 3: The computational time of different methods

Method	Unknowns	Computation time (second)
VIE-based CM in [5]	44338	22087
Formulation in [6]	7326	603
J-formulation in [9]	3663	517
M-formulation in [9]	3663	602
J-formulation in [10]	3663	565
M-formulation in [10]	3663	609
J-formulation in [11]	3663	582
M-formulation in [11]	3663	595
J-formulation in [12]	3663	501
M-formulation in [12]	3663	508
Formulation in [13]	7326	582

similar modal solutions. The existing schemes for CMs of dielectric bodies are cross-verified by the numerical results. The modal solutions given in this paper could serve as benchmarks of CMs for dielectric bodies.

REFERENCES

[1] R. J. Garbacz, "Modal expansions for resonance scattering phenomena," Proceedings of the IEEE, vol. 53, no. 8, pp. 856–864, Aug 1965.

[2] R. Garbacz and R. Turpin, "A generalized expansion for radiated and scattered fields," IEEE Transactions on Antennas and Propagation, vol. 19, no. 3, pp. 348–358, May 1971.

[3] R. Harrington and J. Mautz, "Theory of characteristic modes for conducting bodies," IEEE Transactions on Antennas and Propagation, vol. 19, no. 5, pp. 622–628, Sep. 1971.

[4] R. Harrington and J. Mautz, "Computation of characteristic modes for conducting bodies," IEEE Transactions on Antennas and Propagation, vol. 19, no. 5, pp. 629–639, Sep. 1971.

[5] R. Harrington, J. Mautz, and Yu Chang, "Characteristic modes for dielectric and magnetic bodies," IEEE Transactions on Antennas and Propagation, vol. 20, no. 2, pp. 194–198, March 1972.

[6] Y. Chang and R. Harrington, "A surface formulation for characteristic modes of material bodies," IEEE Transactions on Antennas and Propagation, vol. 25, no. 6, pp. 789–795, November 1977.

[7] H. Alroughani, J. L. T. Ethier, and D. A. McNamara, "Observations on computational outcomes for the characteristic modes of dielectric objects," in 2014 IEEE Antennas and Propagation Society International Symposium (APSURSI), July 2014, pp. 844–845.

[8] Y. Chen and C. F. Wang, "Surface integral equation based characteristic mode formulation for dielectric resonators," in 2014 IEEE Antennas and Propagation Society International Symposium (APSURSI), July 2014, pp. 846–847.

[9] Y. Chen, "Alternative surface integral equation-based characteristic mode analysis of dielectric resonator antennas," IET Microwaves, Antennas Propagation, vol. 10, no. 2, pp. 193–201, 2016.

[10] F. G. Hu and C. F. Wang, "Integral equation formulations for characteristic modes of dielectric and magnetic bodies," IEEE Transactions on Antennas and Propagation, vol. 64, no. 11, pp. 4770–4776, Nov 2016.

[11] R. Lian, J. Pan, and S. Huang, "Alternative surface integral equation formulations for characteristic modes of dielectric and magnetic bodies," IEEE Transactions on Antennas and Propagation, vol. 65, no. 9, pp. 4706–4716, Sep. 2017.

[12] P. Yla-Oijala, H. Wallen, D. C. Tzarouchis, and A. Sihvola, "Surface integral equation-based characteristic mode formulation for penetrable bodies," IEEE Transactions on Antennas and Propagation, vol. 66, no. 7, pp. 3532–3539, July 2018.

[13] P. Yla-Oijala, "Generalized theory of characteristic modes," IEEE Transactions on Antennas and Propagation, vol. 67, no. 6, pp. 3915–3923, June 2019.

[14] L. Guo, Y. Chen, and S. Yang, "Characteristic mode formulation for dielectric coated conducting bodies," IEEE Transactions on Antennas and Propagation, vol. 65, no. 3, pp. 1248–1258, March 2017.

[15] L. Guo, Y. Chen, and S. Yang, "Generalized characteristic-mode formulation for composite structures with arbitrarily metallicâĂŞdielectric combinations," IEEE Transactions on Antennas and Propagation, vol. 66, no. 7, pp. 3556–3566, July 2018.

[16] S. Huang, J. Pan, Y. Luo, and D. Yang, "Single-source surface integral equation formulations for characteristic modes of fully dielectric-coated objects," IEEE Transactions on Antennas and Propagation, vol. 67, no. 7, pp. 4914–4919, July 2019.

[17] Q. Wu, "General metallic-dielectric structures: A characteristic mode analysis using volume-surface formulations," IEEE Antennas and Propagation Magazine, vol. 61, no. 3, pp. 27–36, June 2019.

[18] P. Yla-Oijala, A. Lehtovuori, H. Wallen, and V. Viikari, "Coupling of characteristic modes on pec and lossy dielectric structures," IEEE Transactions on Antennas and Propagation, vol. 67, no. 4, pp. 2565–2573, April 2019.

[19] K. Chen, "A mathematical formulation of the equivalence principle," IEEE Transactions on Microwave Theory and Techniques, vol. 37, no. 10, pp. 1576–1581, Oct 1989.

[20] S. Huang, J. Pan, and Y. Luo, "Investigations of non-physical characteristic modes of material bodies," IEEE Access, vol. 6, pp. 17 198–17 204, 2018.

[21] R. F. Harrington, Time-Harmonic Electromagnetic Fields. McGraw-Hill, 1961.

[22] Q. I. Dai, Q. S. Liu, H. U. I. Gan, and W. C. Chew, "Combined field integral equation-based theory of characteristic mode," IEEE Transactions on Antennas and Propagation, vol. 63, no. 9, pp. 3973–3981, Sep. 2015.

[23] R. F. Harrington, Field computation by moment methods. Wiley-IEEE Press, 1993.

[24] S. Rao, D. Wilton, and A. Glisson, "Electromagnetic scattering by surfaces of arbitrary shape," IEEE Transactions on Antennas and Propagation, vol. 30, no. 3, pp. 409–418, May 1982.

[25] R. K. Mongia, "Theoretical and experimental resonant frequencies of rectangular dielectric resonators," IEE Proceedings H - Microwaves, Antennas and Propagation, vol. 139, no. 1, pp. 98–104, Feb 1992.

[26] D. Kajfez, A. W. Glisson, and J. James, "Computed modal field distributions for isolated dielectric resonators," IEEE Transactions on Microwave Theory and Techniques, vol. 32, no. 12, pp. 1609–1616, Dec 1984.

[27] A. W. Glisson, D. Kajfez, and J. James, "Evaluation of modes in dielectric resonators using a surface integral equation formulation," IEEE Transactions on Microwave Theory and Techniques, vol. 31, no. 12, pp. 1023–1029, Dec 1983.

[28] D. Schaubert, D. Wilton, and A. Glisson, "A tetrahedral modeling method for electromagnetic scattering by arbitrarily shaped inhomogeneous dielectric bodies," IEEE Transactions on Antennas and Propagation, vol. 32, no. 1, pp. 77–85, January 1984.

SHAODE HUANG was born in Sichuan Province, China, in 1992. He received the B.S. degree in electromagnetic field and microwave technique from the University of Electronic Science and Technology of China (UESTC), Chengdu, China, in 2014, and he is currently working toward the Ph.D. degree. His current research interests include antennas theory and computational electromagnetics.

JIN PAN received the B.S. degree in Electronics and Communication Engineering of Radio Engineering Department, Sichuan University, Chengdu, China, in 1983, then M.S. and Ph.D. degrees in electromagnetic field and microwave technique from UESTC in 1983 and 1986, respectively. From 2000 to 2001, he was a visiting scholar in the Electronics and Communication Engineering of Radio Engineering Department, City University of Hong Kong. He is currently a Full Professor in the School of Electronic Engineering, UESTC. His current research interests include electromagnetic theory and computation, antenna theory and technique, field and wave in inhomogeneous media, microwave remote sensing theory and its applications.

CHAO-FU WANG (M'98-SM'02) received the B.Sc. degree in mathematics from the Henan Normal University, Xinxiang, China, in 1985, the M.Sc. degree in applied mathematics from the Hunan University, Changsha, China, in 1989, and the Ph.D. degree in electrical engineering from the University of Electronic Science and Technology of China, Chengdu, China, in 1995.

From 1987 to 1996, he was a Lecturer and then an Associate Professor with the Nanjing University of Science and Technology, Nanjing, China. From 1996 to 1999, he was a Postdoctoral Research Fellow with the Center for Computational Electromagnetics, University of Illinois at Urbana-Champaign. From 1999 to 2001, he was a Research Fellow with the Department of Electrical and Computer Engineering, National University of Singapore (NUS), Singapore. In 2001, he was transferred to the Temasek Laboratories (TL) at NUS, Singapore, as a Research Scientist, where he became a Senior Research Scientist in 2007 and a Principal Research Scientist in 2011. He has been leading TL Propagation and Scattering Group at NUS for many years to successfully conduct and accomplish research programs funded by Singapore Government. He co-authored *Characteristic Modes: Theory and Applications in Antenna Engineering* (Hoboken, NJ: Wiley, 2015). He has published more than 240 journal and conference papers, and filed six international WIPO/PCT patents. His research interests include fast algorithms for computational electromagnetics, scattering and antenna analysis, theory of characteristic modes and its applications, monolithic microwave integrated circuit (MMIC) design and fast EM simulation, fast prediction of EM scattering from large and complex target, efficient electromagnetic compatibility (EMC)/electromagnetic interference (EMI) modeling for practical platform, and EM scattering & antenna measurement.

Dr. Wang successively served the IEEE Singapore Microwave Theory and Techniques (MTT)/Antennas and Propagation (AP) and EMC Chapters as a committee member, Secretary, Treasurer, and Vice-Chairman from 2003-2012. He served as a Chairman of the IEEE Singapore MTT/AP Chapter in 2013. He was a co-recipient of the 2009 Best *Applied Computational Electromagnetics Society (ACES) Journal* Paper Award. He has been actively involved in organizing several international conferences in Singapore. He has served as the Publication Chair of the 2005 IEEE International Symposium on Radio-Frequency Integration Technology (RFIT2005), RFIT2007, RFIT2012, and 2012 IEEE Asia-Pacific Conference on Antennas and Propagation (APCAP2012), the Organizing Committee Secretary of the 2005 IEEE International Workshop on Antenna Technology (IWAT2005) and 2006 International Symposium on Antennas and Propagation (ISAP2006), the Exhibition and Sponsorship Chair of the 2009 Asia Pacific Microwave Conference (APMC2009), the Exhibition Co-Chair of the 2018 Joint IEEE International Symposium on Electromagnetic Compatibility and Asia-Pacific Symposium on Electromagnetic Compatibility (2018 Joint IEEE EMC & APEMC Symposium), and Finance Chair of the IEEE APCAP2018. He is a General Chair of 2020 IEEE International Conference on Computational Electromagnetics (ICCEM 2020) and Special Session Chair of 2021 IEEE International Symposium on Antennas and Propagation and USNC-URSI Radio Science Meeting (IEEE AP-S/URSI 2021). As a regular reviewer of many international journals, he is currently an Associate Editor of the *IEEE Journal on Multiscale and Multiphysics Computational Techniques*, *International Journal of Numerical Modelling: Electronic Networks, Devices and Fields*, and *Electronics Letters*. As a Guest Editor of the *International Journal of Numerical Modelling: Electronic Networks, Devices and Fields*, he edits a special issue on advanced solution methods for modeling complex electromagnetic problems.

This article has been accepted for publication in a future issue of this journal, but has not been fully edited. Content may change prior to final publication. Citation information: DOI 10.1109/ACCESS.2019.2963278, IEEE Access

YUYUE LUO was born in Sichuan Province, China, in 1991. She received the B.S degree in electromagnetic field and microwave technique from the University of Electronic Science and Technology of China (UESTC), Chengdu, China, in 2013, and she is currently a Ph.D. candidate of UESTC. Her current research interests include antenna theory and array signal processing.

DEQIANG YANG received the B.S. degree, the M.S. degree and Ph.D. degree in electromagnetic field and microwave technique from the University of Electronic Science and Technology of China (UESTC) in 1992 ,2006 and 2012, respectively. His current research interests include antenna theory and technique, antenna measurement and development of sensors for UWB system.